· Rejection of backgrounds (θ's etc gamma)

Detection Methods for Gamma Ray Astronomy

Good reference:
Very High Energy Gamma-Ray Astronomy
Trevor Weekes (TC Weekes)
Institute of Physics Publishing, 2003

Why θ's? See Simon Swordy plot.

Three basic energy ranges, set by detection techniques needed, not by physics:

1) Detailed reconstruction of conversions

Photon above Compton/Conversion critical point, but e^+e^- pair lose energy by ~~conversion~~ ionization. SHOW PDG PLOT

SIMON SWARTY PLOT FROM ONG

⇒ undetectable at top of atmosphere, from ground or mountain, can be contained in constructed apparatus.
⇒ fluxes reasonably high (many particles/m^2/s) ← but this is mostly charged, still...
⇒ space-based instrument (GLAST/FERMI) ↑

Charged AX directional. Also, GLAST has anticoincidence detector to remove.

Energy range: 30 MeV - 100 GeV

Above this, shower too penetrating for satellite-borne instrument, and fluxes get too low! However, showers become significant

Cosmic Ray Energy Spectrum

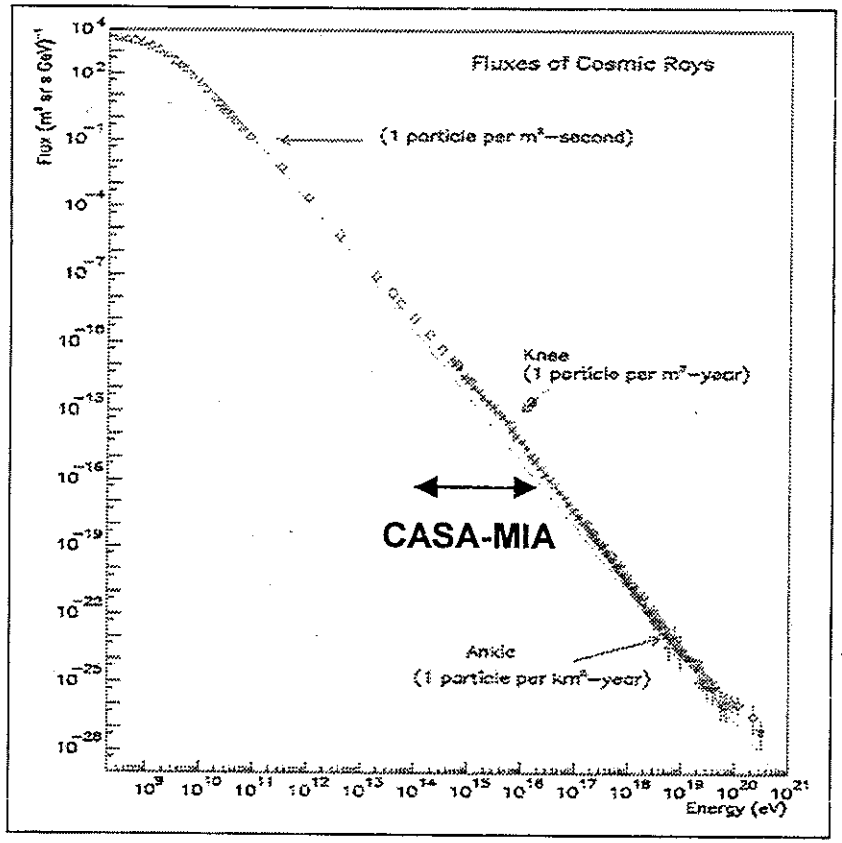

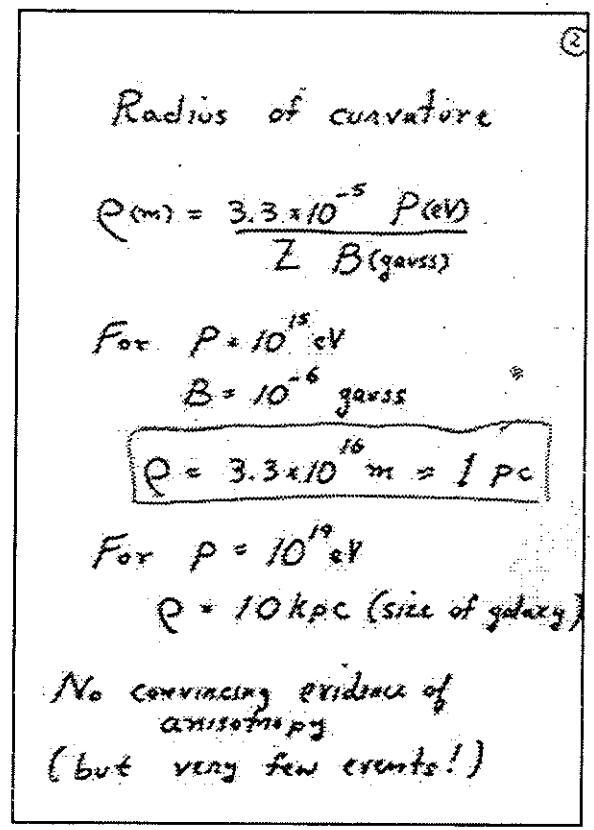

Figure 1: *Left: The cosmic ray energy spectrum. The flux of cosmic rays is shown as a function of energy from* 10^8 *eV to* 10^{21} *eV. The sensitive range of the CASA-MIA experiment is shown by the arrow; figure was originated by S. Swordy. Right: Calculation by Jim Cronin*

Contributions to Photon Cross Section in Carbon and Lead

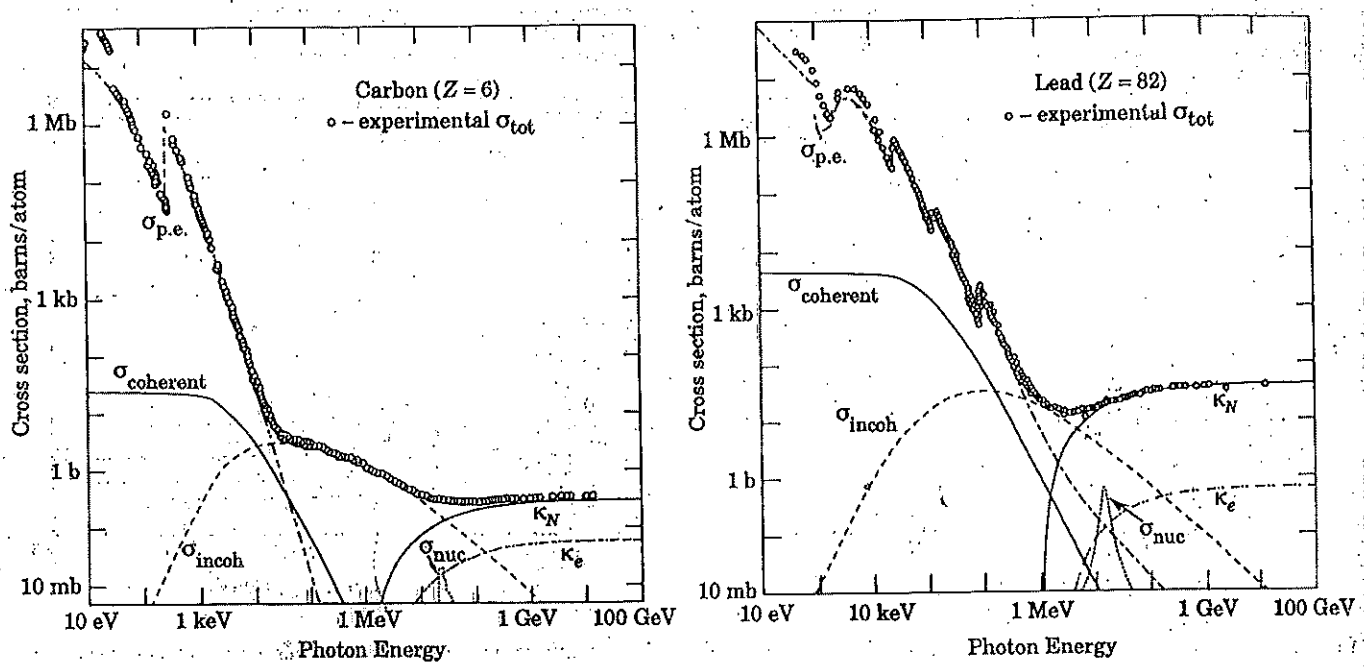

Figure 11.3: Photon total cross sections as a function of energy in carbon and lead, showing the contributions of different processes.

$\sigma_{\text{p.e.}}$ = Atomic photo-effect (electron ejection, photon absorption)

σ_{coherent} = Coherent scattering (Rayleigh scattering—atom neither ionized nor excited)

$\sigma_{\text{incoherent}}$ = Incoherent scattering (Compton scattering off an electron)

κ_n = Pair production, nuclear field

κ_e = Pair production, electron field

σ_{nuc} = Photonuclear absorption (nuclear absorption, usually followed by emission of a neutron or other particle)

From Hubbell, Gimm, and Øverbø, J. Phys. Chem. Ref. Data **9**, 1023 (80). The photon total cross section is assumed approximately flat for at least two decades beyond the energy range shown. Figures courtesy J.H. Hubbell.

Fractional Energy Loss for Electrons and Positrons in Lead

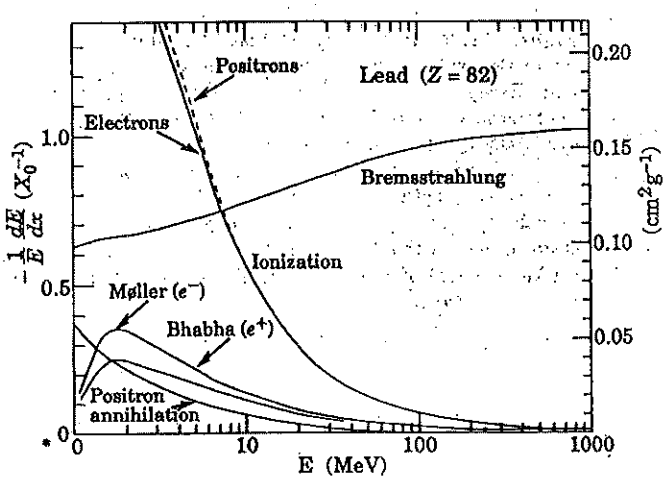

Figure 11.4: Fractional energy loss per radiation length in lead as a function of electron or positron energy. Electron (positron) scattering is considered as ionization when the energy loss per collision is below 0.255 MeV, and as Moller (Bhabha) scattering when it is above. Adapted from Fig. 3.2 from Messel and Crawford, *Electron-Photon Shower Distribution Function Tables for Lead, Copper, and Air Absorbers*, Pergamon Press, 1970. Messel and Crawford use $X_0(\text{Pb}) = 5.82$ g/cm^2, but we have modified the figures to reflect the value given in the Table of Atomic and Nuclear Properties of Materials, namely $X_0(\text{Pb}) = 6.4$ g/cm^2. The development of electron-photon cascades is approximately independent of absorber when the results are expressed in terms of inverse radiation lengths (*i.e.*, scale on left of plot).

2) Ground-based observation of Č light from shower.

We'll dwell on this most and the project for this section will be the development of a crude shower MC.

Relevant energy range is 100 GeV - 100 TeV ($\sim 10^{14}$ eV)

In this region, fluxes are typically <u>one cosmic ray per km² per second</u>, again dominated by charged particles.

Above this, a significant number of charged particles reach the ground

3) Ground-based observation of charged particle fluxes

Range in energy is very broad, 100 TeV = 10^{14} eV, so

$10^{14} - 10^{20}$ eV

$\gamma_{CMB} + p \rightarrow \Delta^+ \rightarrow \begin{cases} p & \pi^0 \\ n & \pi^+ \end{cases}$ $\sim 10^{20}$ eV

With fluxes as low as 1/km²/year!

This is for <u>hadronic</u> scattering off CMB!!

GZK bound: photoproduction off CR background.

$\sim 10^{20}$ eV. Slowing at $\gtrsim 10^{19}$ eV

FERMI has discovered ~100 pulsars. AGN in classification phase; expect theory to follow soon!

Space-based γ-Ray Telescopes 30 MeV - 100 GeV

EGRET (1991-2000)
GLAST/FERMI (2008 -)

Since EGRET is past history, describe FERMI.

SHOW 30 GeV SHOWER PDG PROFILE

P 51 OF WEEKES) → GLAST apparatus

Total of ~10 X_0 contains most of shower

First X_0 is converter region. Very finely instrumented; Si strips w/ ~250 μm pitch

Reconstruct conversion to get angular path from energy ⇒ less scattering ⇒ better resolution.

Electrons shower & absorbed in cesium-iodide calorimeter. Shower penetration degraded resolution at high energy, but 5-10% over most of range.

P 52 of WEEKES

↳ performance of GLAST

	Ang Res (Degrees)	
	EGRET	FERMI
100 MeV	5.8	3.5
>10 GeV	—	<0.15

Note: Fall-off of acceptance for $E_\gamma < 1$ GeV due to background rejection algorithm!

ı of EGRET and GLAST.

	EGRET (achieved)	GLAST (desired)
	20–30 000	20–300 000
	1500	>8000
	0.5	>2
degrees	5.8	3.5
degrees		<0.15
	10	10
')	10^{-7}	
	1	0.06

GRET so it cannot really be classified as

· (AMS)

MS) is a very large and expensive mission
pace Station [1]. Its primary purpose is
ne sensitivity for the study of cosmic ray
nsist of a magnetic spectrometer with large
gnet, layers of silicon tracker, scintillators.
id state Cherenkov detector. For gamma-
ivity similar to that of EGRET. However,
sible to direct the telescope so it will not
pportunity. A preliminary version of the
June, 1998. The AMS is scheduled to go

Space Telescope (GLAST)

lescope (GLAST) is the next-generation
it will replace the spark chamber with
compact, more ...cient, and have better
er, the general principle of the telescope

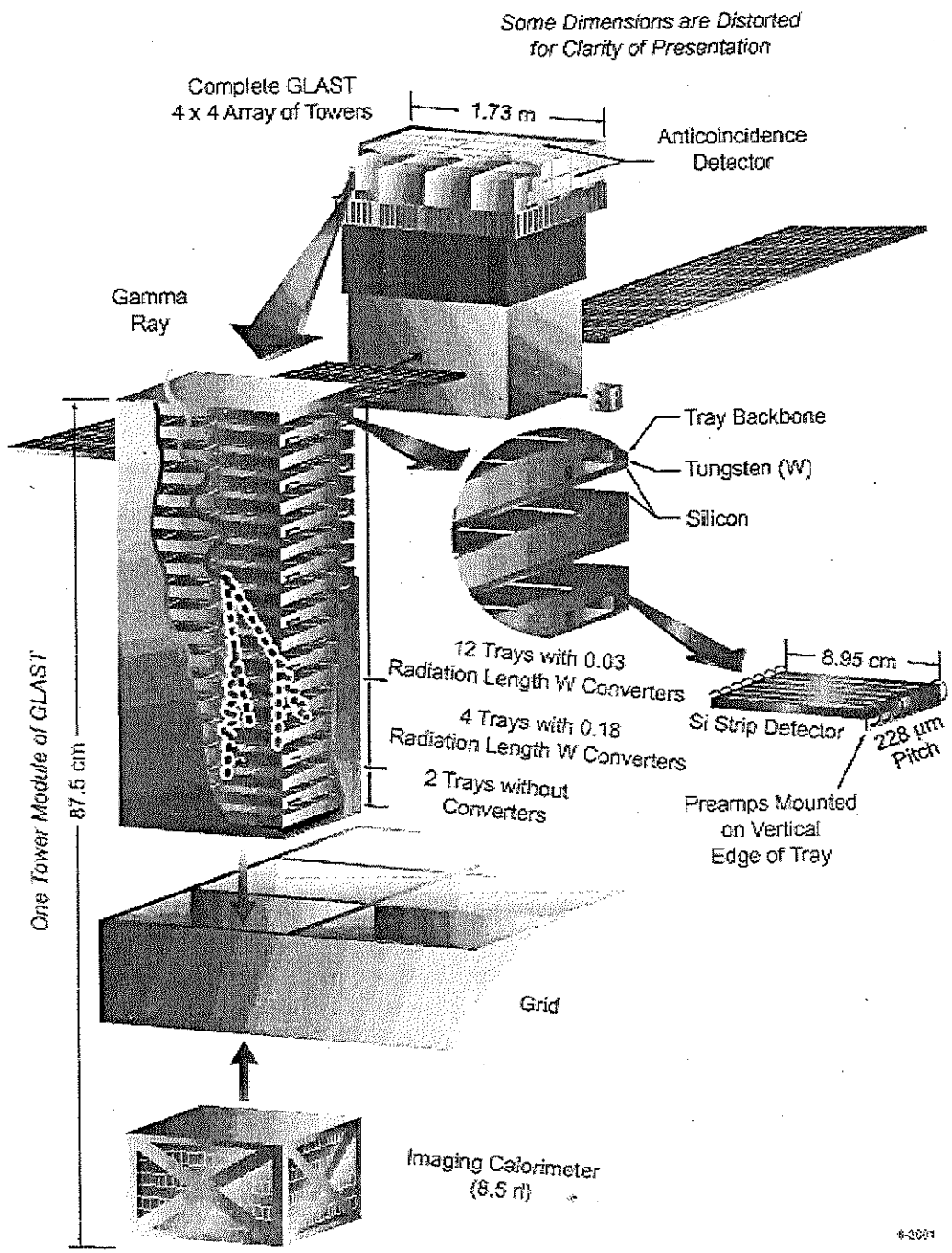

Figure 3.5. A sche... ic diagram of the Large Area Telescope on GLAST showing the

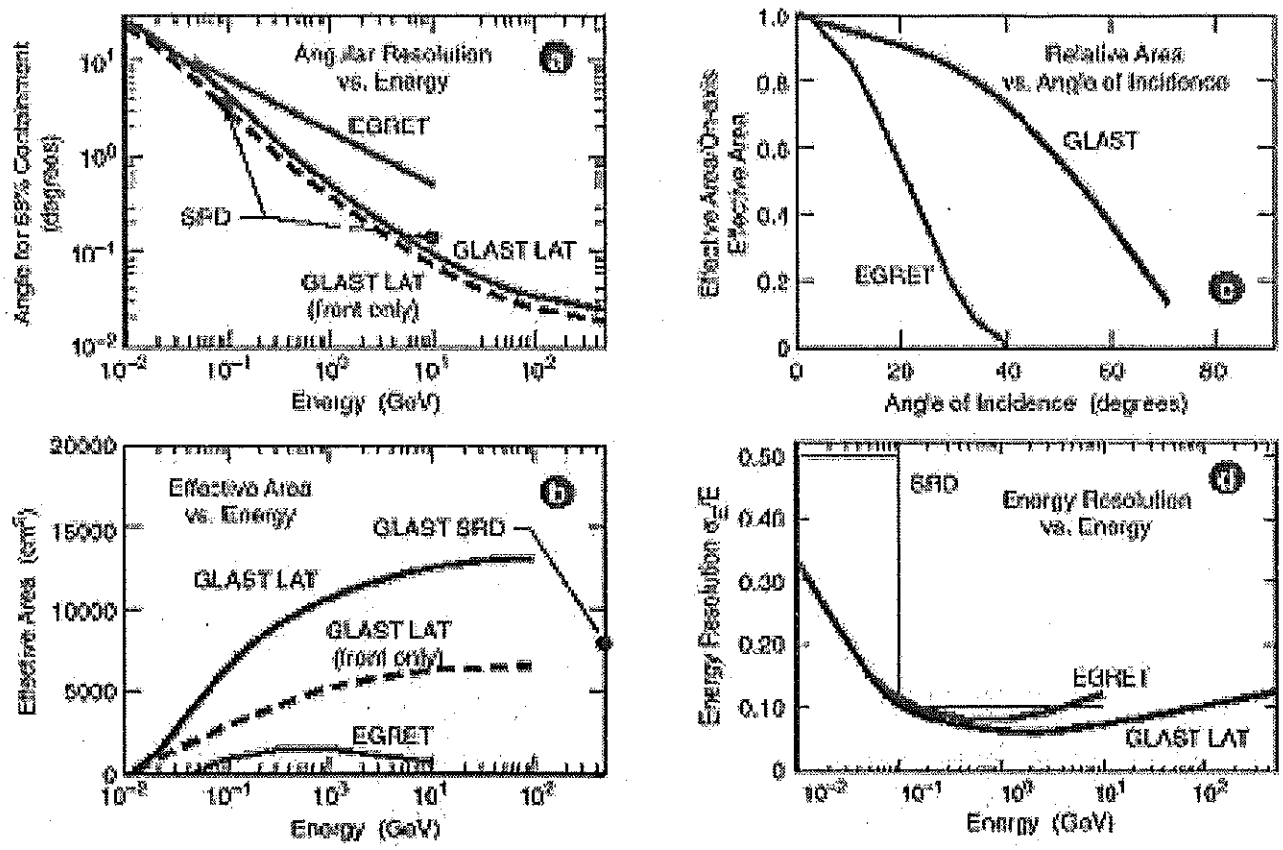

Figure 3.6. GLAST performance predictions as a function of energy compared with EGRET. (http://glast.gsfc.nasa.gov/resources/)

GLAST consists of two parts: the Large Area Telescope (LAT) and the Gamma-Ray Burst Monitor (GRM) [5]. GRM is a simple wide-field low energy instrument to alert GLAST to the occurrence of a gamma-ray burst. LAT has three components (figure 3.5).

(i) The tracker/convertor consists of 18 layers of ionizing particle-sensitive detectors with high Z. They provide the familiar pair production track which is used to distinguish the gamma rays from charged cosmic rays.

(ii) The calorimeter will be made of eight layers of bars of caesium iodide, with individual read-outs to give spatial resolution. The calorimeter will be 8.5 radiation lengths thick which permits the detector to operate with some efficiency up to 300 GeV.

(iii) The anti-coincidence detector is made from tiles of plastic scintillator which are read out through wavelength-shifting fibers and miniature phototubes. This segmented structure reduces self-vetoing due to backscattering from the tracker/convertor.

The telescope has a modular design with 16 individual tracker/converter

Atmospheric Cerenkov Detection 100 GeV - 100 TeV

Atmosphere is (on average) 1030 $g\,cm^{-2}$ of air, with $X_0 = 37.1\ g\,cm^{-2}$ ⇒ almost 28 radiation lengths of air (like 7m of lead!)

Density varies, but depth of one X_0 is about 20km up.

⇒ typical γ ray will convert at 20km

$$\gamma \to e^+e^-$$

e^+, e^- radiate, those photons convert, etc ⇒ SHOWER.

SHOW PDG ENERGY LOSS

For $E_\gamma \approx 1$ TeV, only a handful of charged particles reach ground, even at mountain altitudes.

What is detected?

Note: index of refraction of air at sea level is $n \approx 1.0003$. ⇒ $c = 1/n \doteq 0.9997$

What does it take for an electron to be going faster than the effective speed of light?

$$\gamma \cong \frac{1}{\sqrt{1-\beta^2}} \cong \frac{1}{\sqrt{1-(.9997)^2}} \cong 40$$

Note: E_{crit} in air about ~100 MeV!

$$E = \gamma m \sim 40(\tfrac{1}{2}\,\text{MeV}) \cong 20\ \text{MeV}$$

$$\rightarrow n(P,T) - 1 = (2.7\times10^{-4})\left(\frac{P}{P_0}\right)\left(\frac{T_0}{T}\right)$$

STP

(somewhat larger for upper atmosphere, since density, and thus n, is a bit less).

For showers from >100 GeV conversions, these electrons and positrons will radiate. via Cerenkov enough to be detected from ground.

Note also that

$$\cos\theta_c = \frac{c}{n\cdot v}$$

$\beta = .9997$ when $E_e \sim 20$ MeV! so, $v/c \sim 1$

and so for above threshold, $v \sim c$, and

$$\cos\theta_c \sim \frac{1}{n} \sim .9997$$

This is for forward, $\theta_c \sim 1.3°$ (somewhat less higher up)..

$\Rightarrow$ Č radiation maintains directional information of electron/positron that produced it!

The maximum number of particles produced is then,

$$N_{\max} \simeq \frac{E_0}{E_c} . \tag{2.128}$$

This simple model, however, only gives a rough qualitative picture of the shower. To make a more precise calculation, recourse to such techniques as Monte Carlo simulations is generally required. Figure 2.26 shows the results of one such calculation for a 30 GeV shower in iron [2.15]. The circles and squares essentially give the number of electrons and photons, respectively, as a function of depth in the iron, while the histogram describes the energy deposited by the shower, i.e., dE/dt. As we can see now, the number of particles is an electron-photon cascade rises exponentially to a relatively broad maximum after which it declines gradually over many radiation lengths, rather than stopping abruptly as in the simple model above. It is important to keep in mind here that the calculation describes the *average* behavior of the cascade. As mentioned in Sect. 2.4.2, there can be large fluctuations when bremsstrahlung is involved, so that for any given individual shower, a large deviations from the mean will be observed.

Beyond the first radiation length or so, the energy loss, dE/dt, can be fit reasonably well by the gamma distribution

$$\frac{dE}{dt} = E_0 b \frac{(bt)^{a-1} e^{-bt}}{\Gamma(a)} \tag{2.129}$$

where a and b are parameters dependent on the material. The depth at which the maximum occurs is given by

$$t_{\max} = (a-1)/b = 1.0 \times (\ln y + C_i) \ , \quad i = e, \gamma \tag{2.130}$$

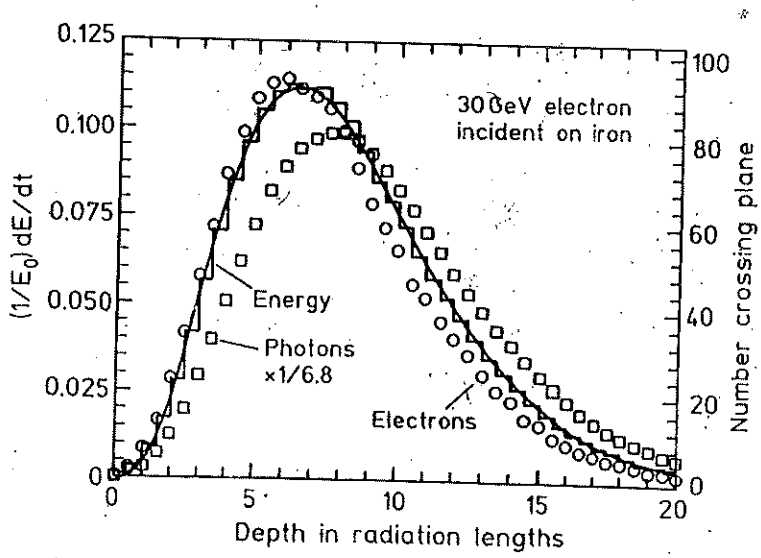

Fig. 2.26. Monte Carlo calculation of a 30 GeV electromagnetic cascade in iron (from [2.15]). The histogram shows the fractional energy deposited by the cascade as a function of depth, t, in the material, while the circles and squares represent the number of electrons and photons, respectively, with energy ≥ 1.5 MeV crossing a plane perpendicular to the longitudinal shower direction at depth t. The smooth curve is a fit of the gamma function in (2.129)

SHOW 30 GeV PDG SHOWER PROFILE AGAIN

Shower max occurs ~5-10 X_0 into atmosphere
⇒ typically at a height of 5-10 km.

Let's look w/ more specificity at the shower from a 1 TeV γ ray.

SHOW P 18 OF WEEK 5 anatomy of a shower

Shower max occurs at about 8.5 km. At this height, $\theta_c \sim 0.7°$ or about ~~[illegible]~~ 12 mrad

$(8.5\,km)(.012) \sim 100\,m$

⇒ light from shower max falls in ring of about 100 m radius.

In addition, there's a focusing effect due to the increase in index of refraction w/ pressure, and thus with decreasing altitude.

yes – diff. in path and c light speed is a tn effect, so increases in time as a difference!

This focusing also happens in time, so for the ~75% of light up to and just beyond shower max, a ~100 m ring of light strikes ground in about a ~1 ns pulse!

AEGO

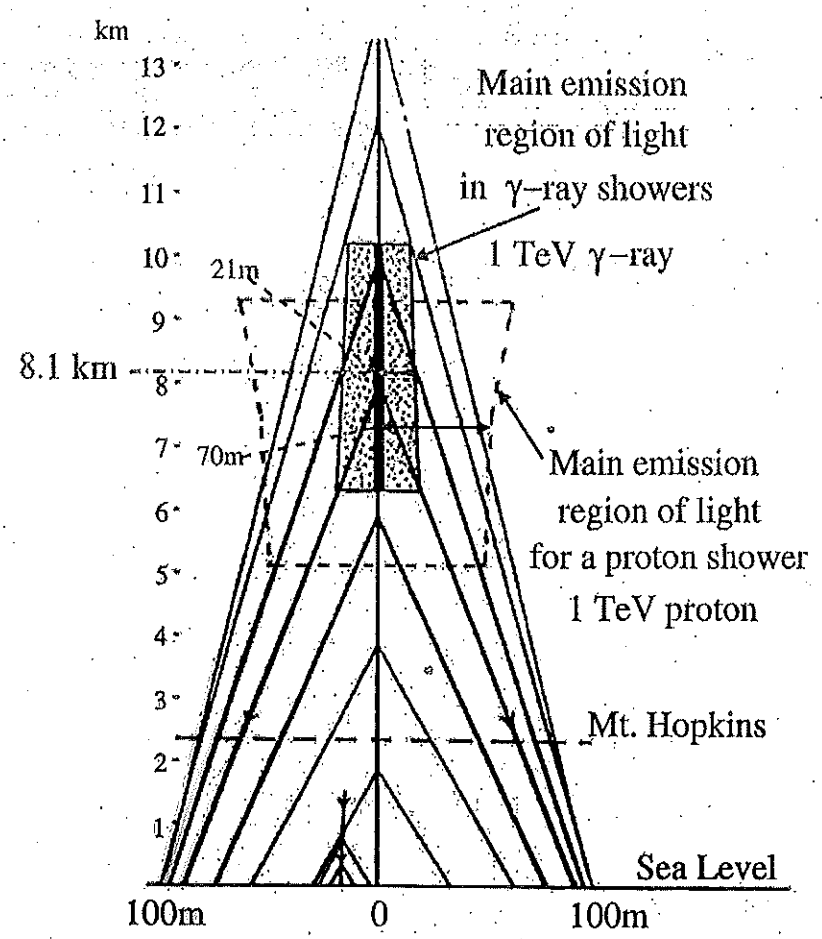

Figure 2.2. Cartoon showing the Cherenkov light emitting regions of gamma-ray and proton air showers. The shaped area corresponds to the main region of emission in a gamma-ray shower of 1 TeV energy. The area enclosed by the broken line is the main region of emission for 1 TeV proton shower. The lateral distribution of light from the gamma-ray shower is shown at the bottom of the diagram. Note that the horizontal scale is magnified by a factor of five [10]. (Figure: A M Hillas.)

2.4 Atmospheric Cherenkov technique

2.4.1 General properties

The basic atmospheric Cherenkov telescope (ACT) can be very simple [25, 4, 19]. First-generation systems consisted of just a single light detector in the focal plane of searchlight mirror coupled to fast pulse counting electronics. The basic elements are illustrated in figure 2.3. Such telescopes are characterized by the mirror collection area, A, the reflectivity, R, the solid angle, Ω, and the integration time, τ. Even with a simple light detector ($A = 2$ m^2, $R = 85\%$, $\Omega = 10^{-3}$, and $\tau = 10$ ns), it is possible to detect the light signal from gamma-ray showers of a few TeV energy with high efficiency. Its identification as coming from a gamma-ray shower rather than from a cosmic ray air shower is quite a different matter

Photons: $\delta = KV_d^{\alpha}$ $0.7 < \alpha < 1.0$
(secondary emission)

The remaining ~25% of light falls inside ring, bunching a bit towards the ~~area~~ middle of the ring, and is subject to large fluctuations since it comes from the shower tail.

Finally, at any point on the ring, the light is extremely <u>directional</u>, with an angular spread of only ~0.2°

⇒ Very good intrinsic information about source location! (20 km away from initial interaction!)

Subtle! You image only if you are on ring (isotropic light ⇒ image everywhere, but Čer light: see full shower only for select angles of emission, ie, on ring!)

γ-Ray Telescopes

SHOW WHIPPLE, WECKES P8
↳ 99.7% rejection of p-showers!

Field of view is 1-2°, matched to 0.2° spread of showers (must know when to look - these are not survey instruments, unlike GLAST/FERMI).

NOTE: Discuss hadronic rejection before arrays.

Light focused onto phototube or similar element, with good (~10-20%) QE and ~1 nsec timing.

Array of sensors is used to provide imaging - sorting out γ from p showers (wait...)

WHIPPLE DETECTOR ARRAY P34 WECKES

important point!

Problem: Are you on ring of moderate shower, or edge of huge shower? ⇒ Energy resolution ⇒ Arrays! (READ)

HESS Array: 4 12m telescopes in Namibia.
Locate ring relative to observation.

{ ME technique
VHE arrays
↳ CASA
↳ AUGER

γ-ray Discrimination and Charged Particle Background

About only 0.1% of HE cosmic rays are photons.
So why bother with them?

For $p = 10^{1.5}$ eV (1000 TeV) and $B = 10^{-6}$ G
(typical intergalactic field)

$$\rho = 3.3 \times 10^{16}\ m \approx 10^{-4} \text{ of } \rho_{galaxy}$$

We ~~[illegible]~~ source identification!
It is important to suppress this background in order to avoid its overwhelming point-source signal from γ's!

Typical γ shower particles: $e^{\pm}, \gamma \Leftarrow p_\perp \sim m_e \sim 1$ MeV/MeV

$p_\perp \sim m_\pi$ (~100 MeV) ⇒ Typical hadron shower particles: $\pi^{\pm} \to \mu\nu$, $\pi^0 \to \gamma\gamma$ ⇒ μ, ν, γ, some π.

$\boxed{\text{p16 of WEEKES}}$

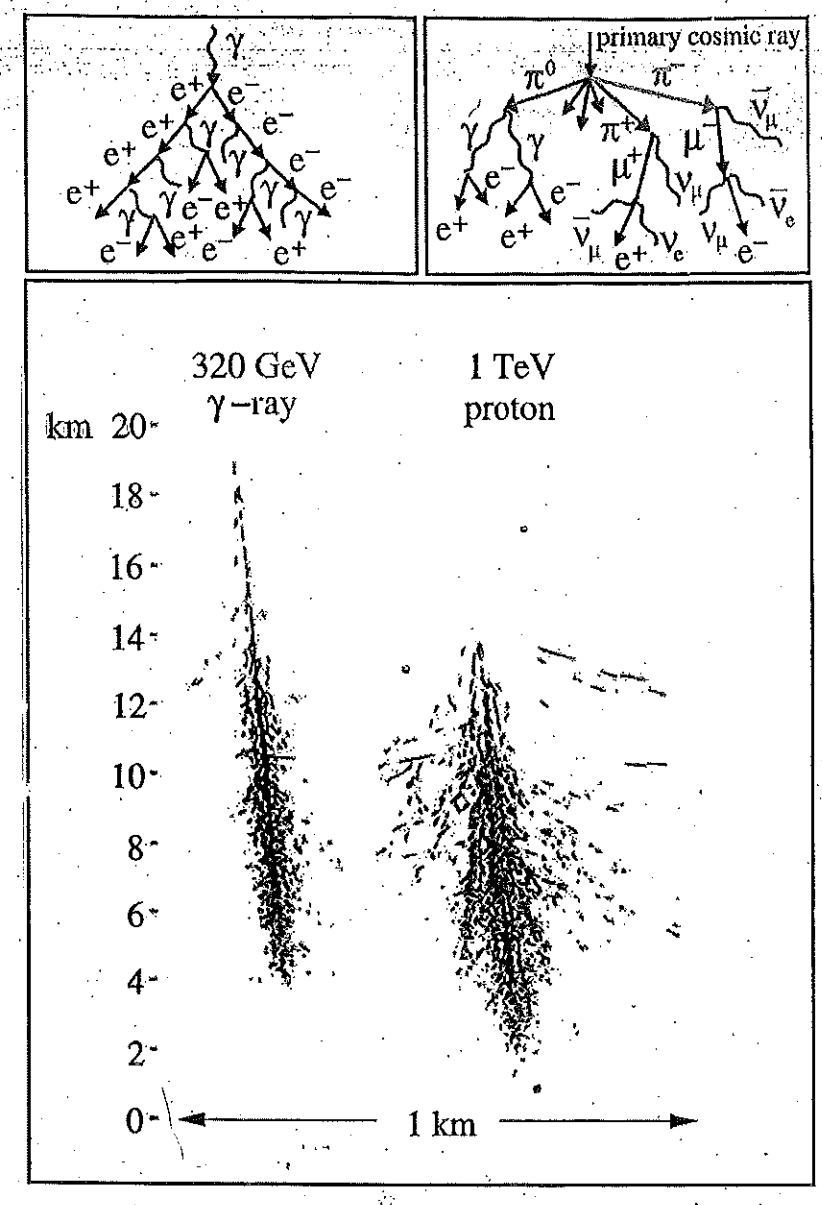

Figure 2.1. Main panel: Monte Carlo simulations of 320 GeV gamma-ray shower and a 1 TeV proton shower. The tracks of Cherenkov light emitting particles are shown but not all to avoid saturation. The horizontal scale is magnified by a factor of five [10]. A schematic development of a gamma-ray shower (left) and a hadronic shower (right) are shown in the two small panels. (Figure: D Horan.)

Cherenkov emission), it is similar to the trail of a meteor. In particular, the column seen on the sky when extrapolated backwards intersects the point of origin of the gamma ray on the cosmic sphere. The optical images of a shower of meteors have a similar property in that they all point back to their point of origin, i.e. the radiant of the meteor shower.

Although the fraction of energy that goes into this optical emission is small (less than 10^{-6} of the primary energy), it is coherent and this makes possible a

Discrimination provided by:

1) Image of shower

2) More penetrating particles ⇒ more closer to ground
   ⇒ less annular (if you have an array of telescopes!)
   ⇒ more in UV, since UV column depth in air less than visible.

3) More spread in time for hadron showers; penetrating particles radiate sooner than straggling electrons at high altitude. { EM shower $e^{\pm}$ only
   Hadron has both

Overall, Whipple has achieved better than 99.7% rejection of charged cosmic rays!

And remember that sources are point-like.

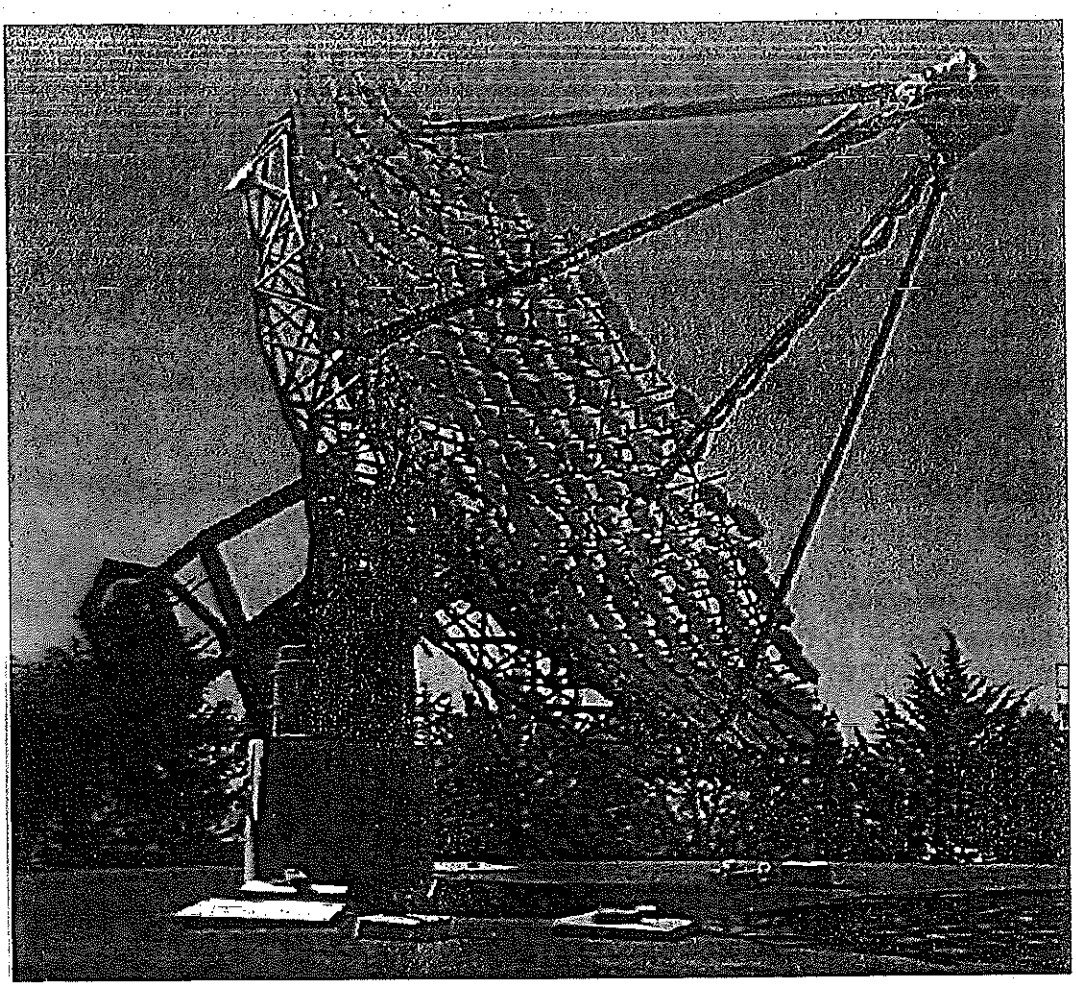

Figure 1.3. The Whipple 10 m gamma-ray telescope. Note the '10 m' refers only to the aperture of the optical reflector; the effective collection area is $>5 \times 10\,000\ \mathrm{m}^2$ so that the gamma-ray 'aperture' is 120 m.

source anomalies in the cosmic ray arrival direction distribution which might point to the existence of discrete sources of VHE cosmic rays. None were found. Not long after the publication of Morrison's seminal paper [9] on the prospects for gamma-ray astronomy at 100 MeV energies (see historical note: seminal paper), Cocconi, a high energy theorist at CERN, produced an equally optimistic prediction for the possibilities of gamma-ray astronomy at VHE energies [5]. He made his predictions for telescopes consisting of arrays of particle detectors. Two such experiments (in Poland and Bolivia) searched for discrete sources but their energy thresholds were high (>100 TeV) and no anomalies were found. Other experimenters realized that the detection of the electromagnetic cascades using the atmospheric Cherenkov radiation was a more sensitive technique and an ambitious array of 12 light detectors was deployed in the Crimea by a group from the Lebedev Institute (figure 1.2). Four years of operation (1960–64) by the Soviet group [3] produced extensive observations of the sources suggested by Cocconi (radio galaxies and supernova remnants) but did not lead to any source

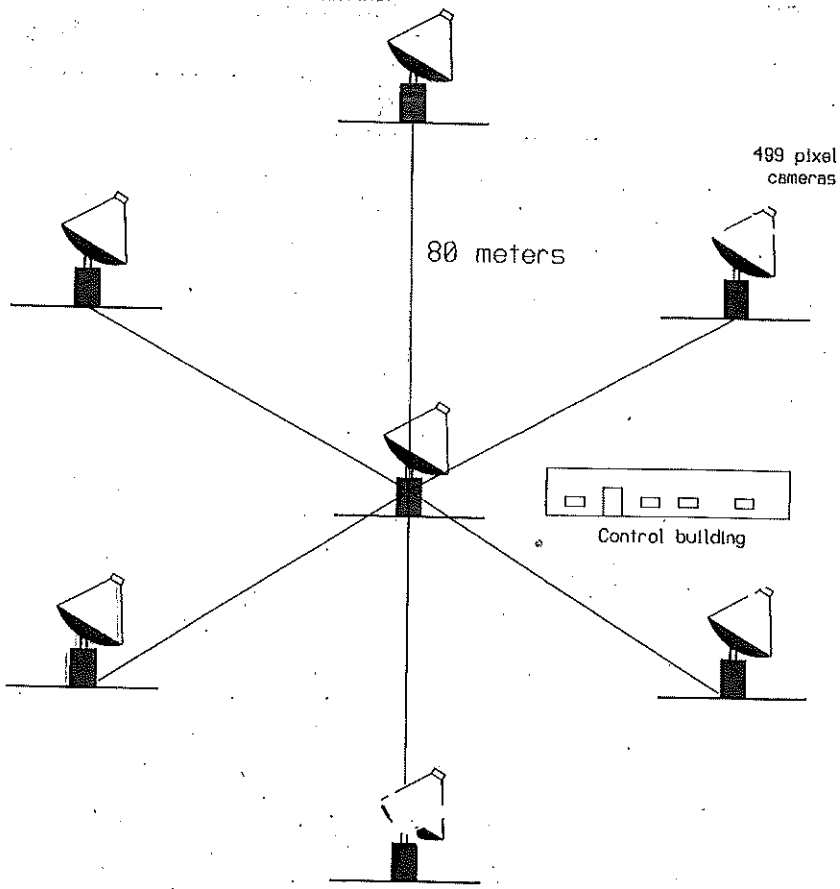

Figure 2.12. The layout of the seven 12 m telescopes that will comprise the VERITAS observatory in southern Arizona.

The Very Energetic Radiation Imaging Telescope Array System (VERITAS) was the first of these next-generation telescopes to be proposed. The seven telescopes in VERITAS will be identical and will have the geometrical layout shown in figure 2.12. Six telescopes will be located at the corners of a hexagon of side 80 m and one will be located at the center. The telescopes will each have a camera consisting of 499 pixels with a field of view of 3.5° diameter. The flux sensitivity of VERITAS (which will be very similar to that of HESS and CANGAROO-III) is given in the next chapter (figure 3.7) where it is contrasted with that of existing telescopes, both ground-based and space-borne.

More by accident than design, the next generation of major new telescopes will have a logical distribution in latitude and longitude with MAGIC and VERITAS in the Northern Hemisphere and HESS and CANGAROO-III in the

Ultra-High Energy (UHE) Arrays - no signals observed yet.

For energies > 100 TeV, flux is small, so must instrument large area + have survey-like coverage.

Small directional collectors not sufficient; instead, can use penetration of particles, particularly at higher elevation.

CASA/MIA : 1/4 km² of scintillation counters

P4 and P6 of ONG (see phzzzl/showers on SCIPP

~1 ns timing allowed determination of angle of wavefront to roughly 1m over 100m

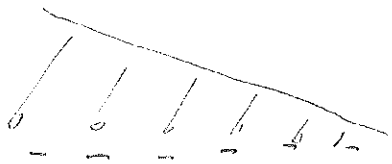

shower profile (dominated by temporal fluctuations in wave-front?) to above limit ~ 0.7° ⇒ good pointing, especially for survey instrument.

GAS MIA : scintillation counters buried under 3m of earth ⇒ detect penetrating μ's and reject hadronic cosmic rays (~94% rejection).

For the very highest energies (10^{20} eV or 10^8 TeV), rates are at ~1/km²/yr, so 1000 km² arrays needed

Auger: 1600 detectors (water ĉ) spaced on 1.5 km grid

⇒ 3000 km².

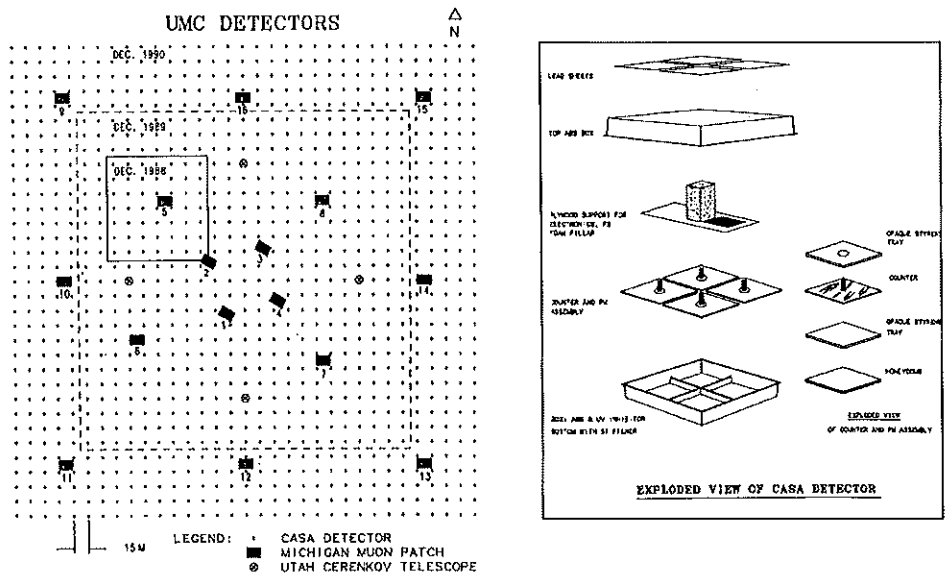

Figure 2: *Left: plan view of the CASA-MIA experiment at Dugway UT, USA, consisting of 1089 surface detectors (CASA), 1024 buried muon counters distributed into 16 patches (MIA), and four small Cherenkov telescopes. Right: exploded view a CASA station, consisting of four scintillation counters enclosed in a water-tight box and covered by four sheets of lead.*

area of 480 m x 480 m. Each detector (or *station*) would consist of four scintillation counters and complete local electronics, encompassing analog, digital, high-voltage, calibration, and Ethernet communication circuitry. CASA would operate in conjunction with a large muon array (MIA), consisting of 512 buried muon counters to be built and installed by the group from the University of Michigan. The NSF proposal was funded and CASA-MIA was constructed as proposed, except that the final CASA was somewhat larger (comprising 1089 detectors) and the final MIA was twice as large (comprising 1024 scintillation counters) as originally proposed.

Full details of the CASA-MIA experiment can be found in a detailed instrument paper written by Jim Cronin [8]. As shown in Figure 2, the 1089 CASA detectors were distributed on a regular grid with a 15 m spacing. The area enclosed by CASA was 0.23 km^2. MIA consisted of 1024 scintillation counters (total scintillator area of 2400 m^2) distributed in 16 patches of 64 counters each. The MIA counters were buried beneath approximately 3 m of earth and had a typical muon energy threshold of $\sim$ 1 GeV.

An exploded view of a single CASA station is shown in Figure 2. The four scintillation counters in each station allowed for local alert (2 out of 4 counters) and trigger (3 out of 4 counters) conditions. Each counter consisted of a square sheet of acrylic scintillator read out by a single photomultiplier tube (PMT) glued to the center of the sheet. The counters were placed in an ABS plastic box, sealed to keep out water and covered by four sheets of lead (1/4" thick), designed to convert the low-energy gamma rays in the shower.

The heart of the CASA experiment was the electronics board mounted on a plywood